Landsvirkjun

LV-2024-085

InSAR monitoring of Krafla, Bjarnarflag and Þeistareykir geothermal areas

2024 update

InSAR monitoring of Krafla, Bjarnarflag and Þeistareykir geothermal areas
2024 update

Höfundur
Vincent Drouin

Dagsetning
November 2024

Lykilsíða

Skýrsla LV nr	LV-2024-085	**Dagsetning**	November 2024
Fjöldi Síðna	30	**Upplag**	1
Dreifing	[ ] Birt á vef LV	[X] Opin	[ ] Takmörkuð til [Dags.]
Titill	InSAR monitoring of Krafla, Bjarnarflag and Þeistareykir geothermal areas. 2024 update		
Höfundar/fyrirtæki	Vincent Drouin / Bylgjuvíxl		
Verkefnisstjóri	Anette K. Mortensen		
Unnið fyrir	Landsvirkjun		
Samvinnuaðilar	–		
Útdráttur	Synthetic Aperture Radar Interferometry (InSAR) of Sentinel-1 images was used to estimate the deformation at Krafla, Bjarnarflag, and Þeistareykir between summer 2023 and summer 2024. Results shows a circular subsidence (~15 mm) within the Krafla caldera. This is the first time since 2018 that such a deformation pattern is observed. The deformation at Bjarnarflag is still stable, at 5-6 mm/yr of subsidence since 1990. At Þeistareykir, the slow subsidence (<5 mm/yr) observed north of Bæjarfjall since the onset of production in 2017 is still ongoing. Similarly, the faster subsidence (10-15 mm/yr) localized near the re-injection boreholes is also constant. However, on the north part of Bæjarfjall itself, the subsidence appears to have accelerated since 2022. The broad inflation pattern first observed between 2022 and 2023 in the Þeistareykir central volcano was still ongoing between summer 2023 and summer 2024, in accordance with GNSS measurements. The uplift is centred near an ancient crater row, ~2 km west of the power station.		
Lykilorð	InSAR, Krafla, Bjarnarflag, Þeistareykir, geothermal, volcano, inflation, subsidence		

Samþykki verkefnisstjóra
Landsvirkjunar

Anette K. Mortensen

Contents

Glossary

ascending orbit When the satellite moves from south to north direction.

descending orbit When the satellite moves from north to south direction.

GNSS [Global Navigation Satellite System] Constellation of satellites providing positioning on a global basis. For instance, GPS.

InSAR [SAR interferometry] Technique consisting in looking at the phase difference between two SAR acquisitions to get information about the ground motion.

LOS [Line-of-sight] InSAR provides deformation measurements along the line-of-sight of the SAR satellite. This means these are one-dimensional deformation measurement, away or toward the satellite, unlike for instance GNSS measurements which are three-dimensional (East, North, Up).

near-East Estimation of the deformation along the East direction, derived from combining multiple LOS deformation.

near-Up Estimation of the deformation along the Up direction, derived from combining multiple LOS deformation.

SAR [Synthetic Aperture Radar] Technique consisting in using the motion of the radar instrument to improve resolution.

1 Introduction

Krafla and Þeistareykir are two active volcanic systems located in the northern part of the Northern Volcanic Zone of Iceland. There are active geothermal fields within both system. These geothermal fields are currently utilised by Landsvirkjun, the National Power Company of Iceland, to produce electricity and direct heating.

The Krafla power station began production in August 1977 with an initial capacity of 30 MW which was extended to 60 MW in 1999. The Bjarnarflag power station, located 8 km SW of the Krafla power station, has been in service since 1969 and has a capacity of 5 MW since 2019 (3 MW earlier). Both power stations are located along the same fissure swarm. A large rifting event with multiple dike intrusions took place within the Krafla volcanic system from 1975 to 1984 (Einarsson, 1991). A magma reservoir located beneath Leirhnjúkur, in the center of the caldera, inflated and deflated multiple time during this event. Following the end of the Krafla Fires in 1984, the magma chamber continued to inflate until 1989. It then started to deflate at a fast rate that quickly slowed down until no movements were visible in the late 1990's (Sturkell et al., 2008). From then on until 2018, the deformation in the area was dominated by subsidence within the Krafla and Bjarnarflag geothermal fields and by subsidence along the fissure swarm (Drouin et al., 2017). Between summer 2018 and summer 2020 a $\sim$11 mm/yr uplift was observed between Leirhnjúkur and the power station (Drouin, 2020).

The Þeistareykir power station began production in November 2017 and has a current capacity of 90 MW. InSAR measurements since the early 1990's show that two inflation events appear to have taken place within the Þeistareykir volcanic system, the first one around 1995 and second one around 2007 (Metzger and Jónsson, 2014). No significant deformation within the geothermal field north of Bæjarfjall was observed prior to the start of production. Between summer 2017 and summer 2020, a localized subsidence of about 5 mm/yr is observed between the power station and Bæjarfjall (Drouin, 2020). The subsidence reaches about 15 mm/yr in the vicinity of the injection wells. A broad uplift, with 12-15 mm/yr velocities at its center, started in 2023 in a similar location as previous inflations in the areas (Drouin, 2023).

2 Data & methodology

Interferometric Synthetic Aperture Radar (InSAR) is a remote sensing technique that allows measurements of surface deformation over large areas. It has been successfully used to observe surface deformation caused by earthquakes, volcanoes, plate tectonics, landslides, glaciers, geothermal utilization, ground-water extraction, etc.

The InSAR principle is to use the phase information of two SAR acquisitions and calculate their difference to generate an interferogram. This interferogram contains various signals: topography, satellite orbits, ground deformation, atmospheric disturbances, and noise. It is possible to extract the deformation signal with time-series analysis. The deformation in the line-of-sight (LOS) of the satellite (i.e. away or toward the satellite) is obtained. An interferogram decorrelates (i.e. loses signal) in areas where the ground surface changes too much between acquisitions. The most common causes are vegetation changes, snow, new constructions, or extremely large deformations. In North Iceland, snow is a main issue, therefore only summer acquisitions (from early June to end of September) are used for InSAR.

There have been many public and commercial SAR satellite missions since the early 1990's. The Sentinel-1 SAR mission (late 2014 - present) is one of the most recent missions and it has been extremely valuable for the InSAR community by providing free-of-charge consistent acquisitions over most of the world. Over Iceland, it provided images every 12 days between 2015 and 2017, every 6 days between 2017 and 2021. Since late December 2021, one of the two Sentinel-1 satellites failed and acquisitions are back to a 12 days repeat time. Each image covers about 240 km wide swath, divided in three sub-swaths of about 80 km. The resolution of a pixel is about 3 m x 14 m.

The images were pre-processed with the Interferometric synthetic aperture radar Scientific Computing Environment, ISCE, (Rosen et al., 2012) before doing the deformation time-series analysis with a in-house implementation of the small-baseline algorithm, SBAS (Berardino et al., 2002). Acquisitions with loss of signal because of snow or with strong atmospheric noise were removed from the analysis.

Three Sentinel-1 tracks covering the areas of interest were analyzed: two tracks on a descending orbits (T9 and T111) and one track on an ascending orbit (T147). The number of images used in the time-series analysis of each of these tracks can be found in Table 1.

Each track has a different point of view over the area of interest. That means it is possible to combine them to extract the East and Up components of the deformation, called near-East and near-Up, respectively, to show the approximation of the decomposition process (Drouin and Sigmundsson, 2019). The North component of the deformation cannot be retrieved because of the near-polar orbits of the satellite.

Table 1: Number of acquisitions selected per summer for each track.

Track	2015	2016	2017	2018	2019	2020	2021	2022	2023	2024	Total
T9	7	7	18	16	18	17	15	11	10	8	**127**
T111	9	8	18	16	16	17	13	9	10	7	**123**
T147	8	7	17	17	19	14	12	10	10	10	**124**

3 Results

3.1 Krafla

The deformation between summer 2023 and summer 2024 shows a circular subsidence pattern within the Krafla caldera (Fig. 1). The maximum of subsidence, about 15 mm/yr, is located in the center of the caldera between Leirhnjúkur and Krafla mountain (Fig. 1b). This is the first time since 2018 that such a clear subsidence signal is observed in the center of the caldera. This subsidence is easier to interpret when compared to the velocities prior to 2018 inflation (Fig. 2a). The deviation/difference between these background velocities and the following years velocities shows a large uplift in the caldera during 2018-2019 (Fig. 2b) and slower uplift between 2019 and 2023 (Fig. 2b-f). And for 2023-2024, the subsidence pattern is clearly visible and is faster than during the reference 2015-2018 background velocities (Fig. 2g). These four phases can also be observed of the time-series plot (Fig. 3): subsidence during 2015-2018, uplift during 2018-2019, stable during 2019-2023, and fast subsidence during 2023-2024. A wide subsidence signal is also visible south-east of the caldera.

At Hvíthólar, it is difficult to distinguish a deformation pattern during 2023-2024 because of the other wider signals (Fig. 2). However, the time-series of vertical deformation at this location shows that it was subsiding similarly to 2015-2017, 2018-2019, and 2021-2023 (Fig. 4). There was little to no vertical deformation during 2017-2018 and 2020-2021. There was uplift during 2019-2020. These temporal variations of the vertical deformation showed a strong correlation with the extraction rate at borehole KJ-21, the main production well in this area (Drouin, 2022). When geothermal fluids are extracted, there was subsidence and when no extraction occurs, there was minor uplift or no significant vertical deformation.

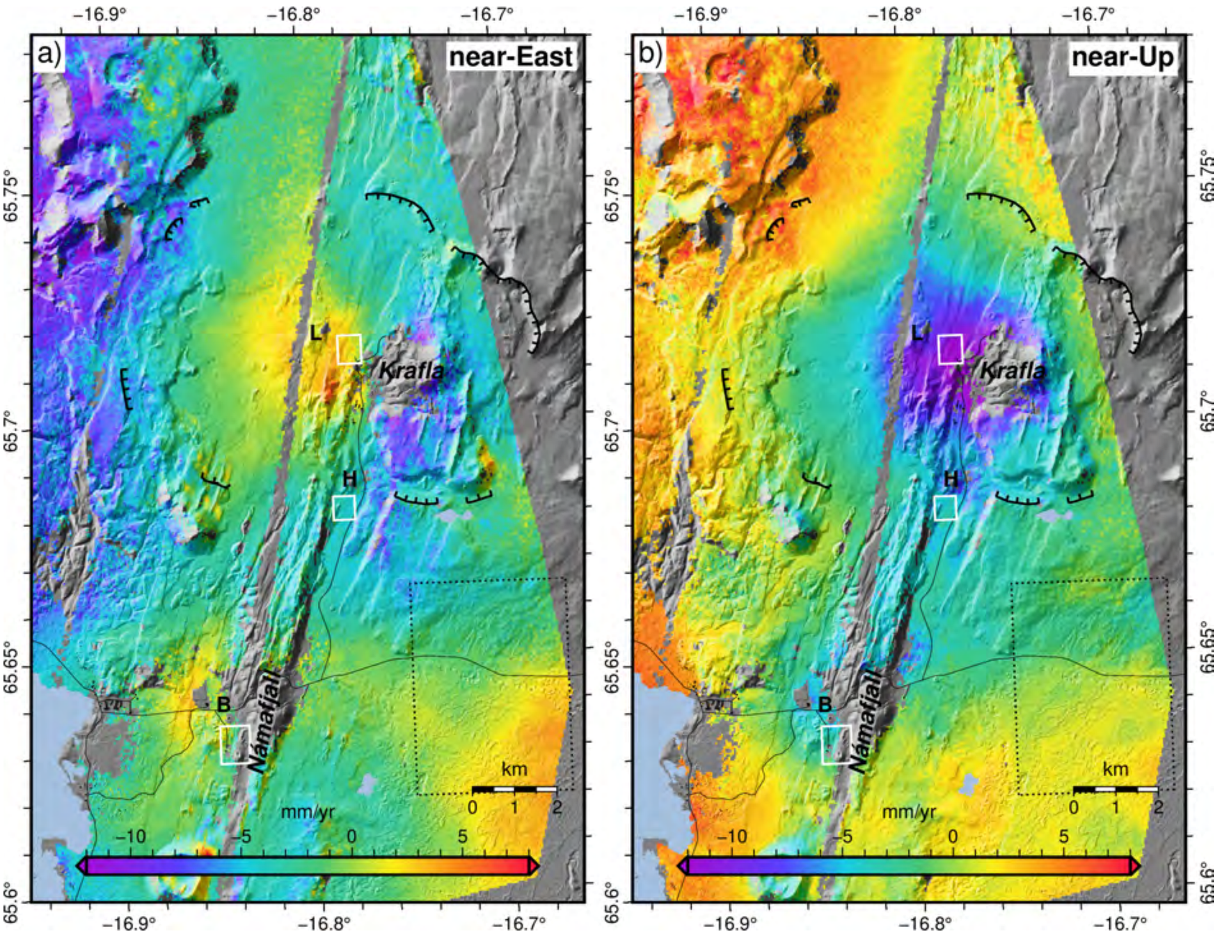

Figure 1: **(a)** Near-East and **(b)** near-Up velocities [mm/yr] between summer 2023 and summer 2024. Leirhnjúkur (L), Hvíthólar (H), and Bjarnarflag are indicated. White boxes show sampling areas for the time-series plots. Velocities are referenced to the area delimited by the dotted line. The North-South line with no data across the velocity fields is caused by a low coherence area at the junction between two image swathes. The exact cause for this issue is not know but it is likely the result of a difference in acquisition geometry between the 2017 reference image and the 2024 images. Background shows shaded topography, the Krafla caldera boundary (comb line), roads (thin lines), and lakes (blue areas).

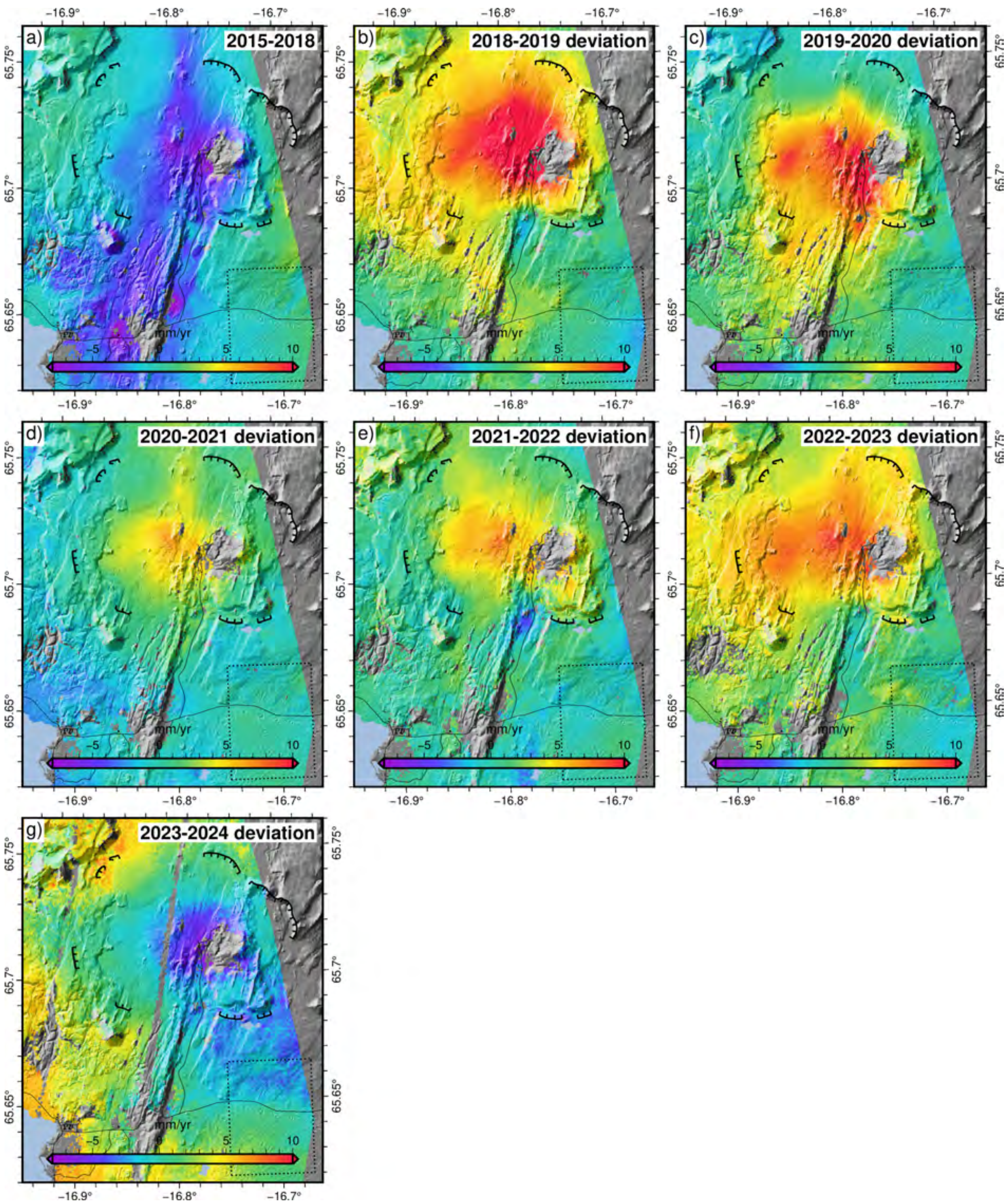

Figure 2: **(a)** Near-Up velocities [mm/yr] for 2015-2018 and **(b-g)** the deviation from it for the following summer-to-summer velocities. Velocities are referenced to the area delimited by the dotted line. Background shows shaded topography, the Krafla caldera boundary (comb line), roads (thin lines), and lakes (blue areas).

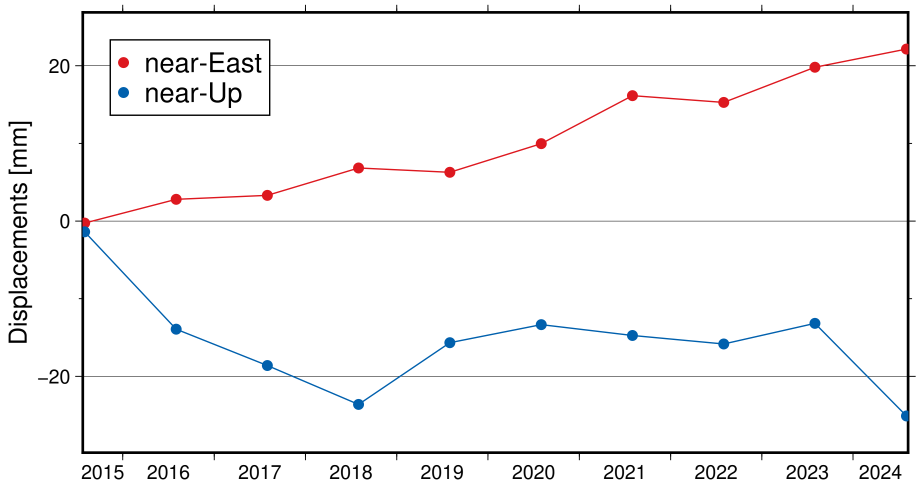

Figure 3: Near-East and Near-Up time-series of deformation near the maximum of uplift during 2018-2020. Location is indicated by the white box between Leirhnjúkur and Krafla on Figure 1.

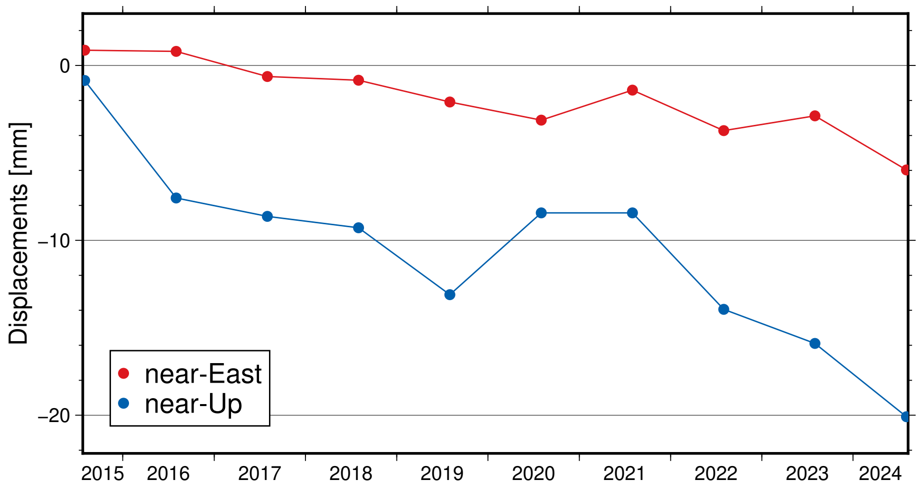

Figure 4: Near-East and Near-Up time-series of deformation near the maximum of uplift during 2018-2020. Location is indicated by the white box next to Hvíthólar on Figure 1.

3.2 Bjarnarflag

Subsidence has been has been fairly constant at Bjarnarflag since 2015, at a rate of about 5-6 mm/yr (Fig. 5). The maximum of subsidence is located west of Bjarnarflag (Fig. 1). There is no change in deformation before and after the inflation at Krafla (Fig. 2).

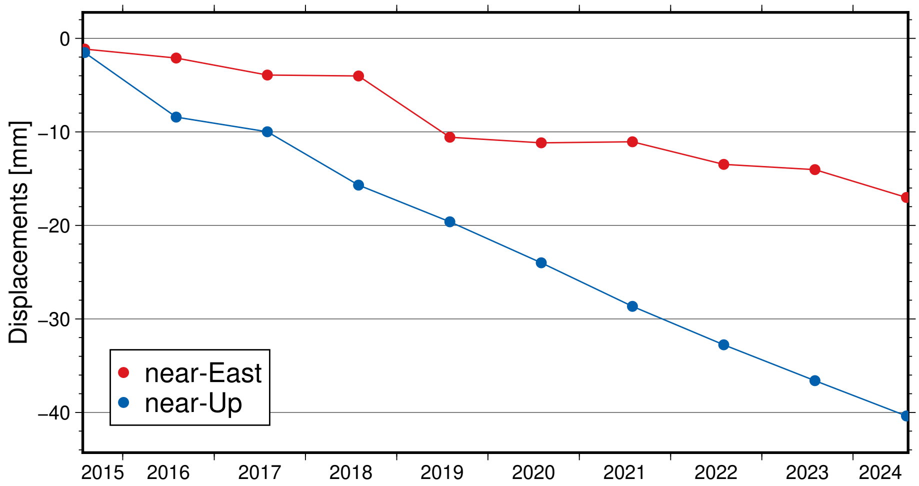

Figure 5: Near-East and Near-Up time-series of deformation at Bjarnarflag. Location is indicated by the white box west of Námafjall on Figure 1.

3.3 Þeistareykir geothermal field

Between summer 2023 and summer 2024, the deformation at Þeistareykir is similar to the 2022-2023 deformation when a broad uplift started (Fig. 6, see Section 3.4 for more details). However, when focusing on the Þeistareykir geothermal field and its immediate surroundings the deformation is similar to what has been observed since 2017 (Fig. 7). A 3-4 mm/yr subsidence is visible in the geothermal field, with a local maximum of about 10 mm/yr. As reported previously, the subsidence appears to be bound on the west side by the Tjarnarás fault. However, the deformation is not as clearly bound on the east side by a fault along Ketilfjall as before. The Tjarnarás fault is also clearly visible on the near-East velocities (Fig. 8). The subsidence extends approximately from the power station in the north to the middle of Bæjarfjall in the south. There, on the north part of the top of Bæjarfjall, the subsidence rate was slow ($\sim$2 mm/yr) until 2022 but has increased to $\sim$7-8 mm/yr since. The fastest subsidence is localized in the north-western part of the geothermal field at the location of three injection wells (ÞN-1, ÞN-2, ÞR-12). There, the subsidence rate has been constant since 2018 (Fig. 11, see Section 3.5 for more details.).

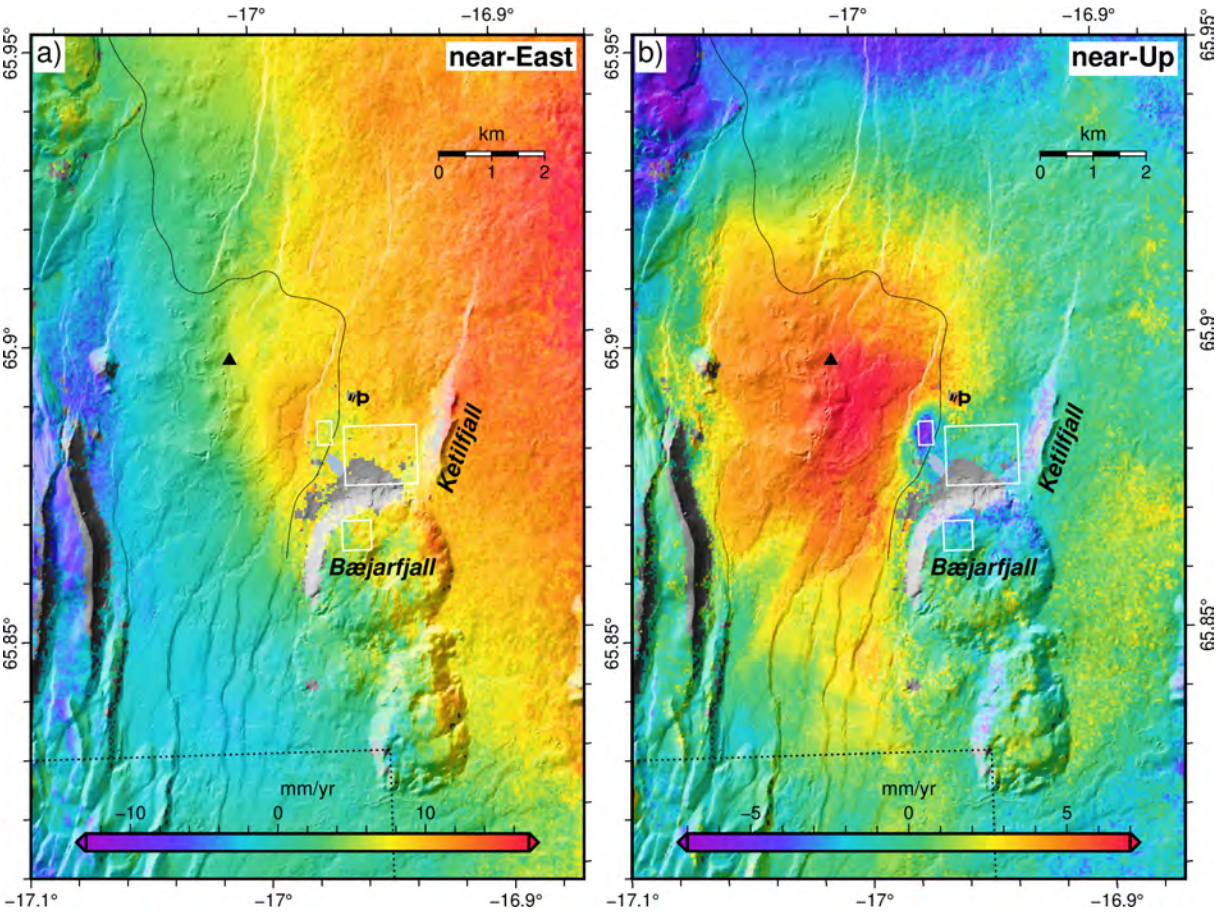

Figure 6: **(a)** Near-East and **(b)** near-Up velocities [mm/yr] between summer 2023 and summer 2024. Þeistareykir power station (Þ) is indicated. The white boxes show the sampling area for the time-series plots. Velocities are referenced to the area delimited by the dotted line. Background shows shaded topography, the THRC continuous GNSS site (black triangle), and roads (thin lines).

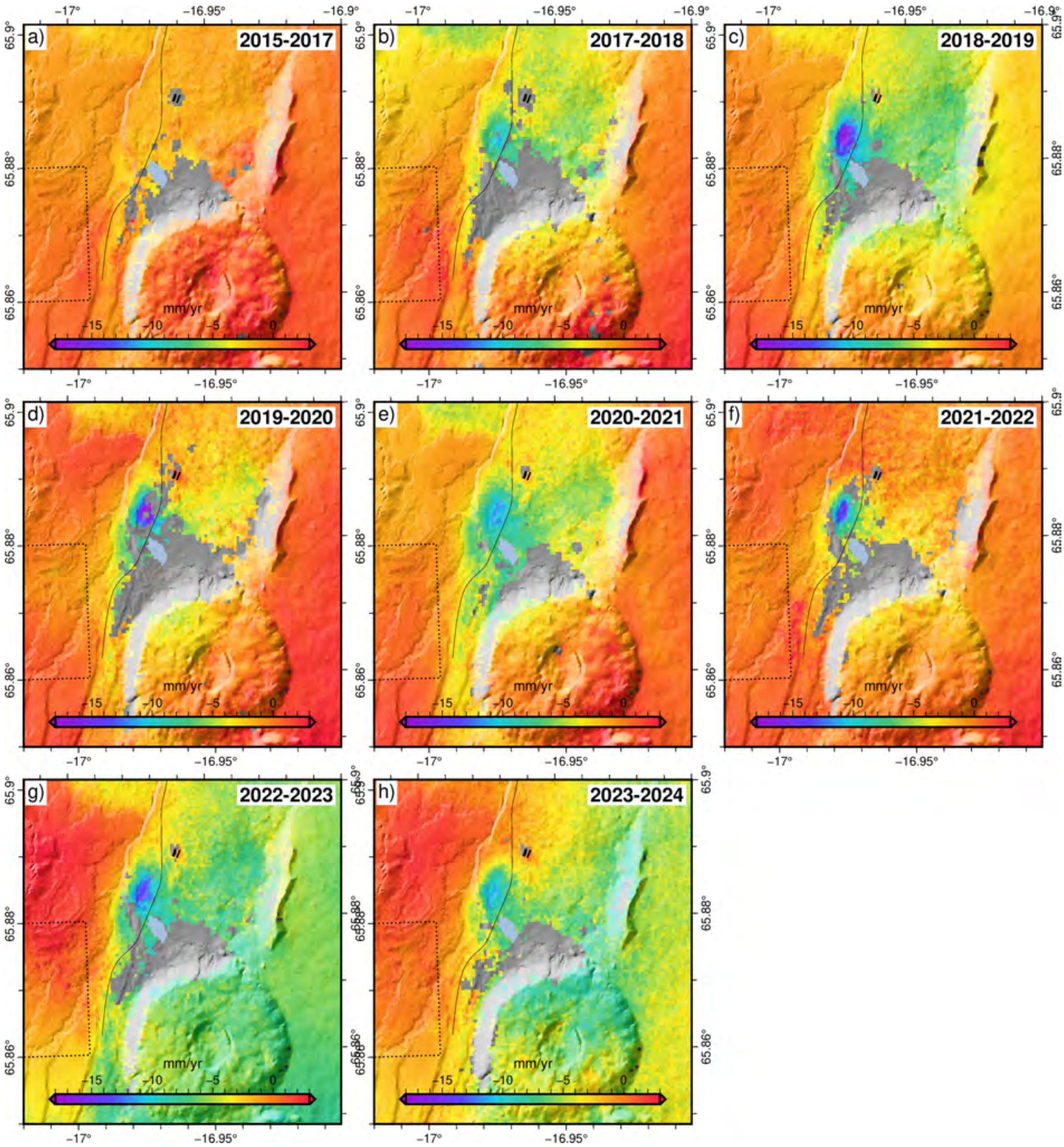

Figure 7: **(a)** Near-Up velocities [mm/yr] prior to production and **(b-h)** summer-to-summer velocities during production. Velocities are referenced to the area delimited by the dotted line. Background shows shaded topography and roads (thin lines).

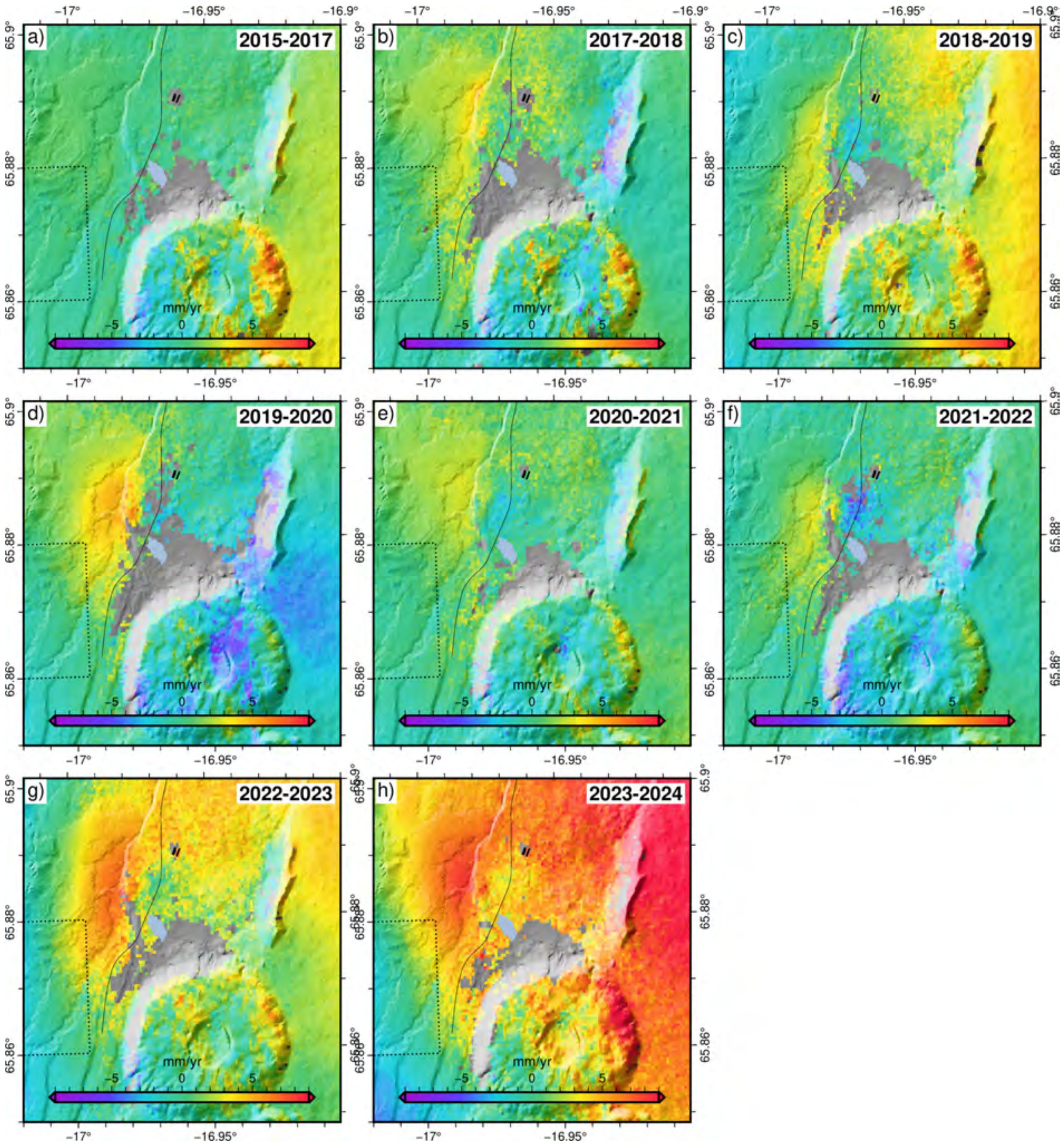

Figure 8: **(a)** Near-East velocities [mm/yr] prior to production and **(b-h)** summer-to-summer velocities during production. Velocities are referenced to the area delimited by the dotted line. Background shows shaded topography and roads (thin lines).

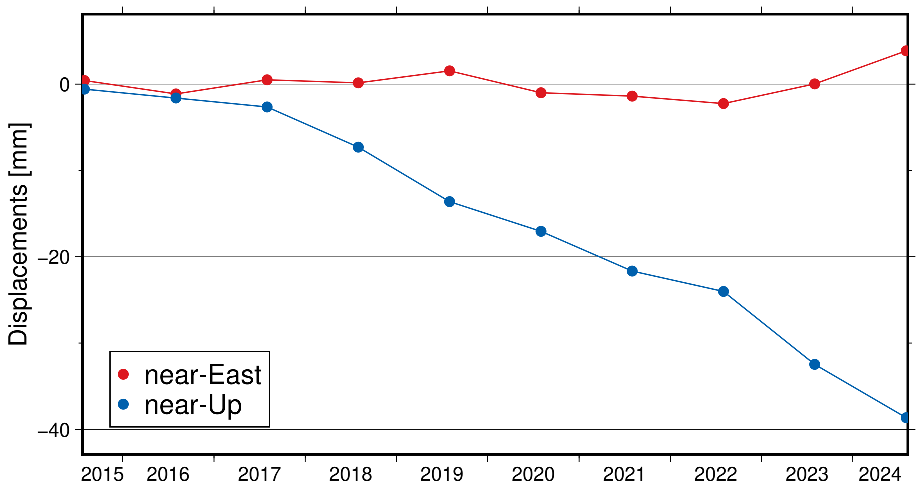

Figure 9: Near-East and Near-Up time-series of deformation north of Bæjarfjall. Production started in 2017. Location is indicated by the larger white box north of Bæjarfjall on Figure 6. Displacements are referenced to the area delimited by the dotted line on Figure 7.

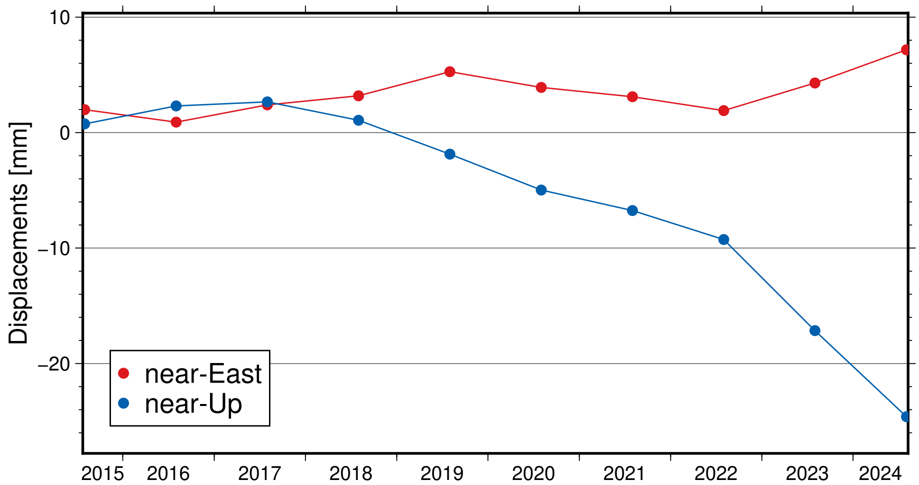

Figure 10: Near-East and Near-Up time-series of deformation at the top of Bæjarfjall. Production started in 2017. Location is indicated by the small white box the top of Bæjarfjall on Figure 6. Displacements are referenced to the area delimited by the dotted line on Figure 7.

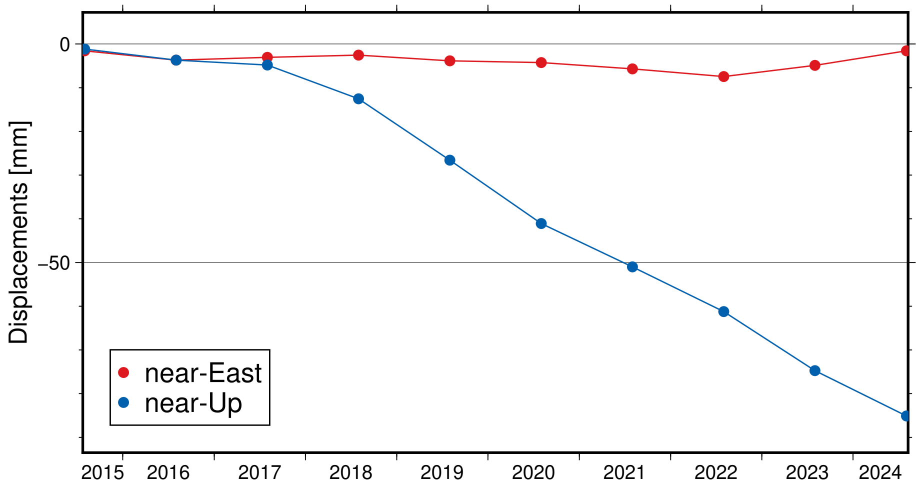

Figure 11: Near-East and Near-Up time-series of deformation at the maximum of subsidence. Production started in 2017. Location is indicated by the smallest white box on Figure 6. Displacements are referenced to the area delimited by the dotted line on Figure 7.

3.4 Þeistareykir central volcano

A broad uplift is visible in the 2023-2024 velocities (Fig. 6). It is a continuation of the uplift that was visible on the 2022-2023 velocities (Drouin, 2023). This uplift becomes very clear when looking at the deviation of the 2022-2024 velocities with respect to the 2017-2022 velocities (Fig. 12). The uplift is ∼10-12 mm/yr between summer 2022 and summer 2024 (Fig. 13). Based on the visual inspection of the near-Up velocities, the center of the uplift is at about -17.007° longitude, 65.8905° latitude (ISN93: 590868, 600718) (see location on Fig. 12). This is a very similar location to the ones found for the center of the source behind previous inflation events (Drouin, 2023; Metzger and Jónsson, 2014). The continuous GNSS site THRC, operated by the University of Iceland, is close to the center of the uplift and shows that uplift started around the beginning of 2023 and stopped around the end of 2023 (appendix Fig. 24). Therefore, the total uplift can be estimated to ∼20-24 mm based on the InSAR velocities.

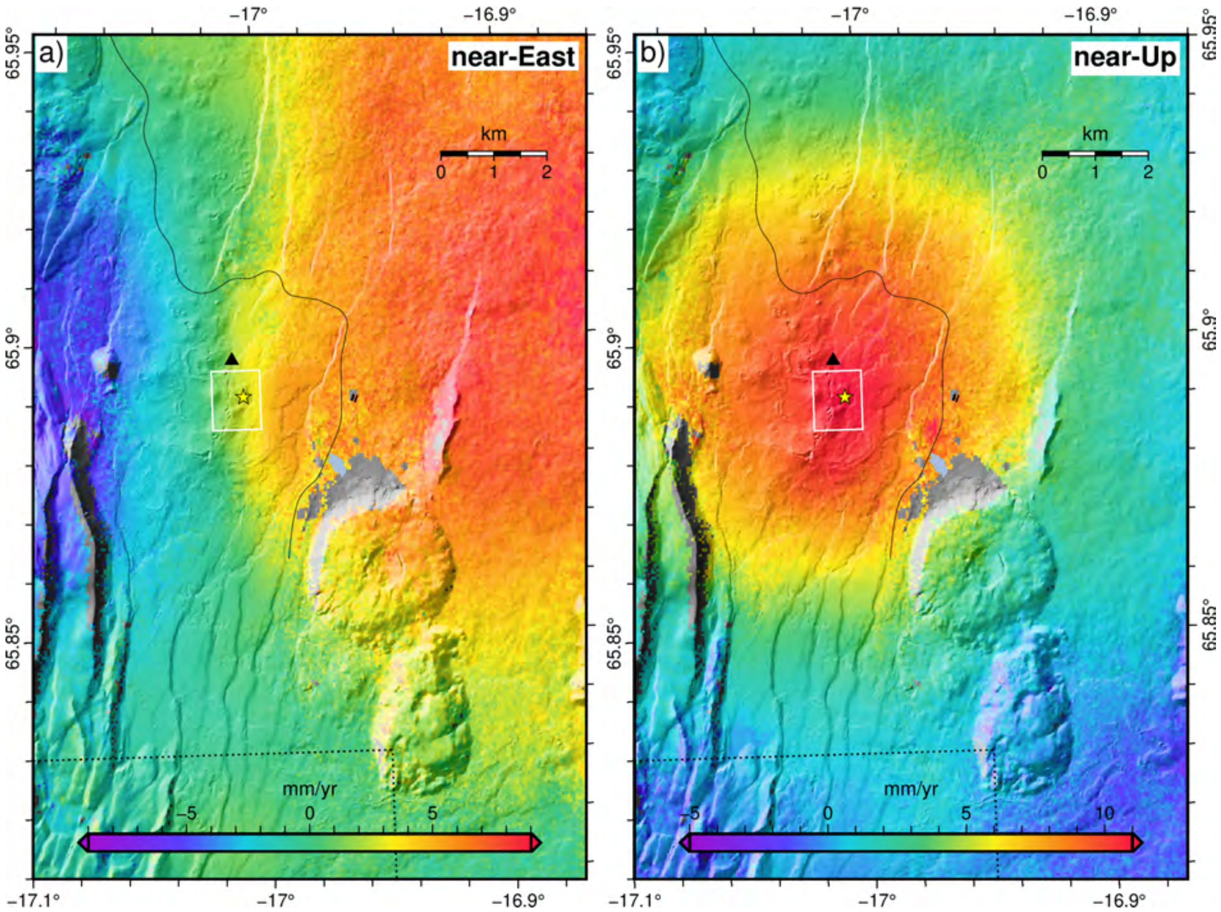

Figure 12: **(a)** Near-East and **(b)** near-Up velocities [mm/yr] of the difference between the 2017-2022 and 2022-2024 time spans. Velocities are referenced to the area delimited by the dotted line. The white box show the sampling area for the time-series plot. Background shows shaded topography, the center of uplift (yellow star), the THRC continuous GNSS site (black triangle), and roads (thin lines).

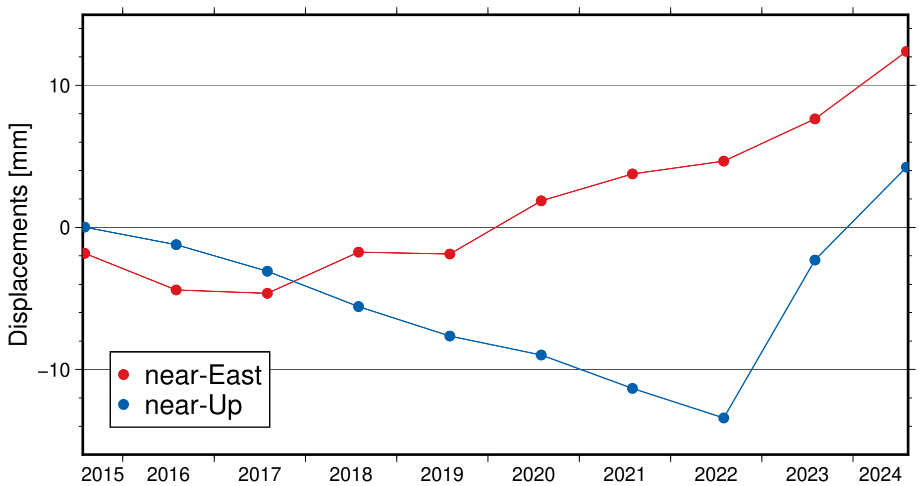

Figure 13: Near-East and Near-Up time-series of deformation at the maximum of the 2022-2024 uplift. Location is indicated by the white box on Figure 12.

3.5 Subsidence at injection boreholes

The peak subsidence at the injection borehole has been fairly stable since the beginning of production (Fig. 11). We created two profiles across the yearly velocities to investigate the potential variations of the deformation pattern between years. One profile goes North-South (NS) and the other goes West-East (WE) (see locations on Fig. 14). Results show that subsidence is very similar through time across the NS and WE profiles (Fig. 15 and 16). After 2018, there are some variations between years but most of it can be attributed to the uncertainty of the velocities. The WE profile is asymmetrical, there is more subsidence to the East than to the West. This is because the east side is within the broader subsidence area of the geothermal field while the west side is across the Tjarnarás fault. On the near-East velocities, no deformation signal is visible along the NS profile (Fig. 17) while a clear contraction signal is visible along the WE profile after 2018 (Fig. 18). These are the expected signals from a subsidence source. Overall, the subsidence pattern appears very stable since 2018.

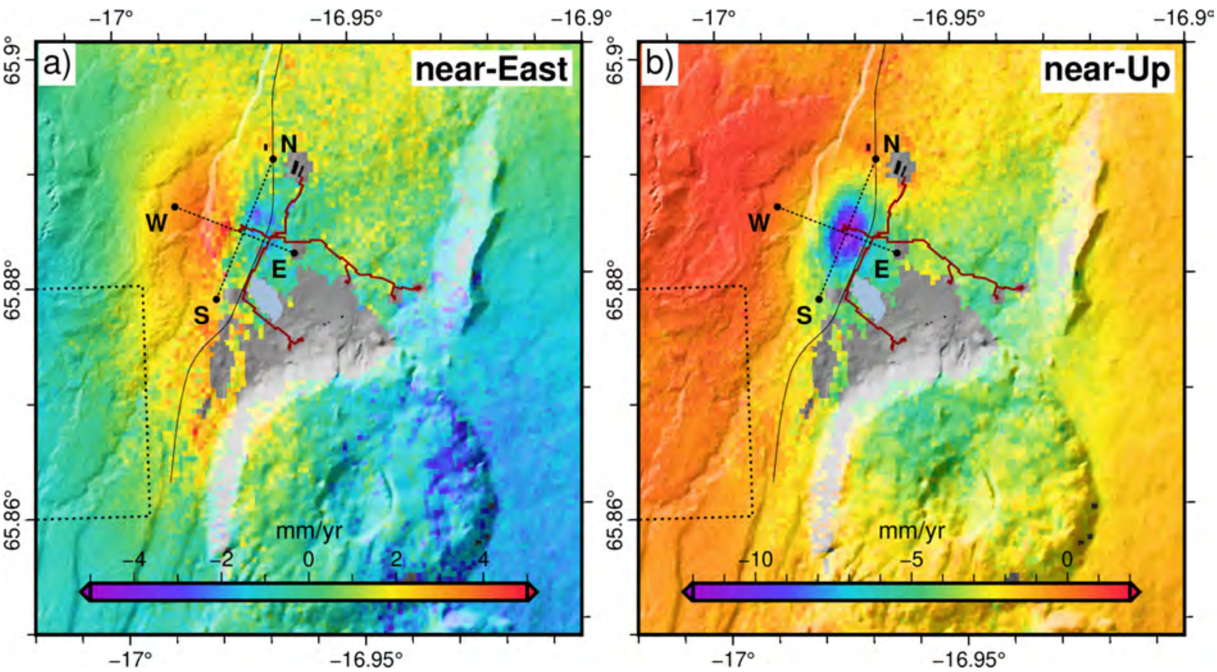

Figure 14: **(a)** Near-East and **(b)** near-Up velocities [mm/yr] of the difference between the 2015-2017 and 2017-2024 time spans. Velocities are referenced to the area delimited by the dotted line. Dashed lines show profiles North-South (NS) and Weast-East (WE) profiles. Background shows shaded topography, roads (black lines), pipelines (red lines), buildings (dark grey areas), and water (blue areas).

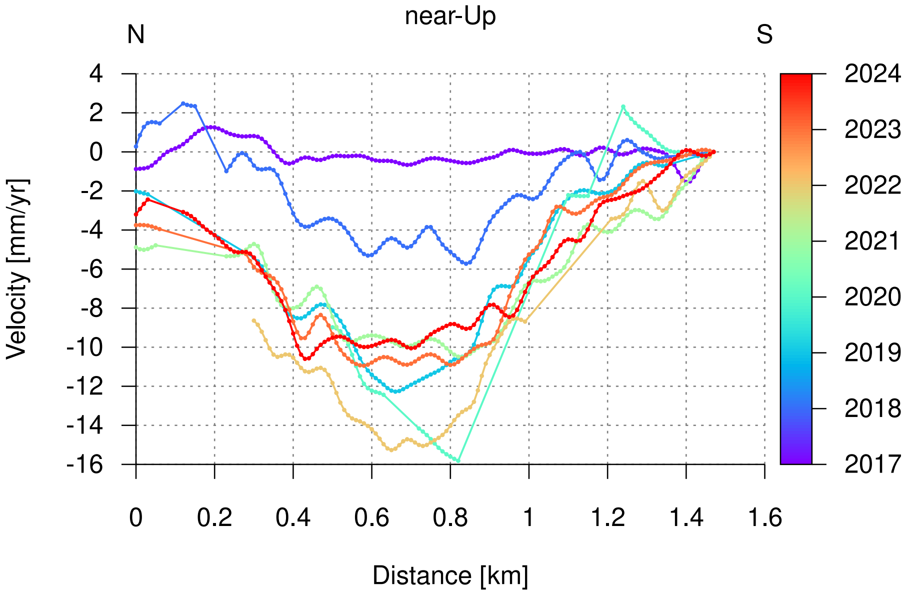

Figure 15: North-South profile across the yearly near-Up velocities. The color scale shows the end year of the yearly velocity. For example, 2024 shows the summer 2023 to summer 2024 velocities. Only 2017 shows the average velocities over two years, from summer 2015 to summer 2017. Velocities are reference to the South end.

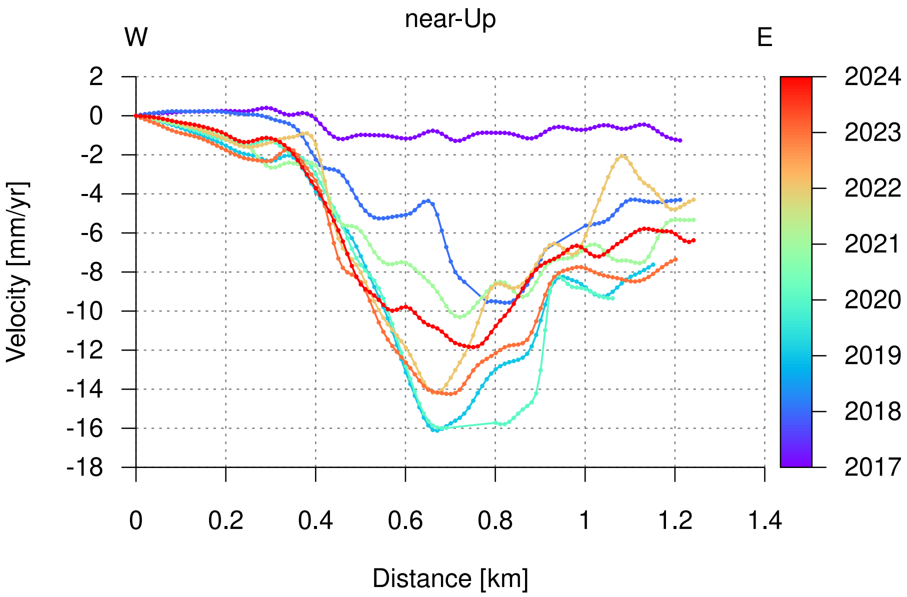

Figure 16: West-East profile across the yearly near-Up velocities. The color scale shows the end year of the yearly velocity. For example, 2024 show the summer 2023 to summer 2024 velocities. Only 2017 shows the average velocities over two years, from summer 2015 to summer 2017. Velocities are reference to the West end.

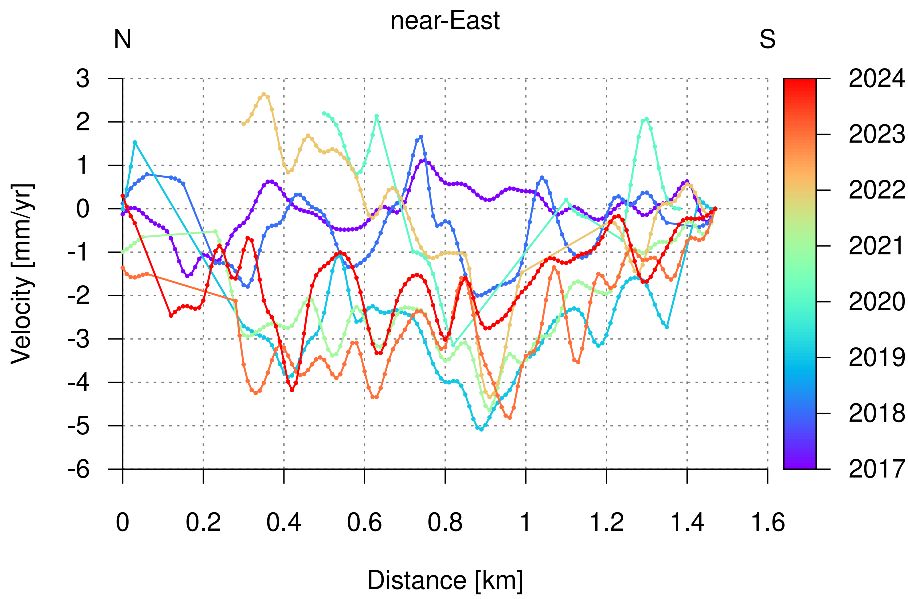

Figure 17: North-South profile across the yearly near-East velocities. The color scale shows the end year of the yearly velocity. For example, 2024 shows the summer 2023 to summer 2024 velocities. Only 2017 shows the average velocities over two years, from summer 2015 to summer 2017. Velocities are reference to the South end.

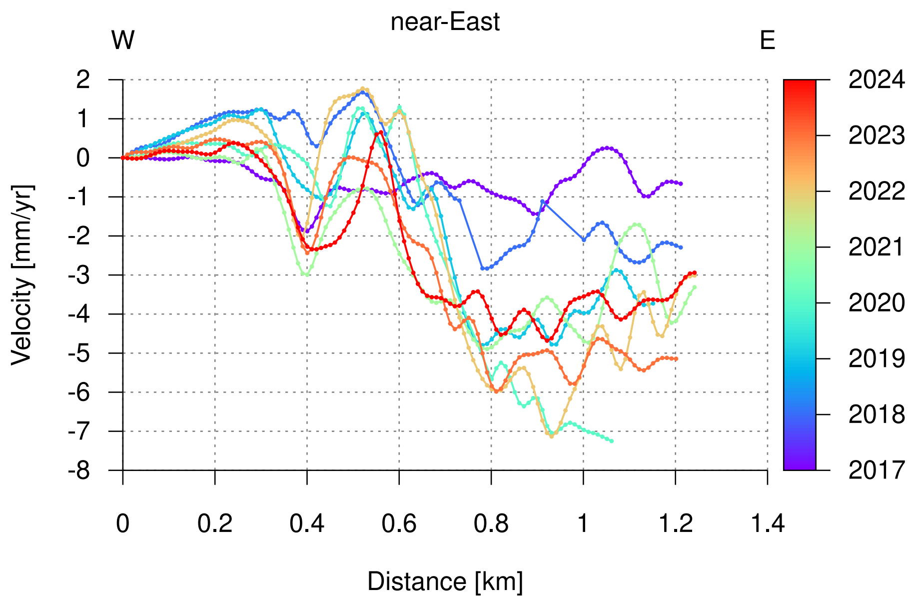

Figure 18: West-East profile across the yearly near-East velocities. The color scale shows the end year of the yearly velocity. For example, 2024 show the summer 2023 to summer 2024 velocities. Only 2017 shows the average velocities over two years, from summer 2015 to summer 2017. Velocities are reference to the West end.

3.6 Retrieving deformation signal in geothermally altered areas

In this report and previous reports it is noticeable that no deformation information was retrieved in the center of each geothermal areas. These zones correspond to areas where the ground was altered by geothermal activity and their surface is mostly made of soft clay with little to no bedrock exposed. This is problematic for measuring deformation using InSAR as the ground needs to have good and stable reflectors for the technique to works.

Two main InSAR analysis techniques exist:

- PS-InSAR: the technique identifies stable natural reflectors, called permanent scatterers (PS), from time-series (Ferretti et al., 2000, 2001). These PS are usually identified at the pixel resolution.
- SBAS (Small Baselines Subset): this technique focus on forming only interferograms close in time and space to minimize the loss of signal cause by both (Berardino et al., 2002). Then to further improve the signal to noise ratio, the interferograms are usually down-sampled by averaging many pixels together.

In this report and previous reports we have used the SBAS technique as it usually gives better results in non-urban areas, like Krafla and Þeistareykir. Unfortunately, as experience has shown, this techniques does not work well on geothermally altered ground. On the other hand, the PS-InSAR technique works on the full resolution image and can identify PS very well on man-made structures (buildings, roads, ...) and other isolated PS like boulders or rock outcrops. We therefore investigated if this technique could identify good PS on the pipelines, well heads, and potential isolated rocks in these geothermally altered areas. Only the first step of the technique to identify good PS was carried out. It consists in looking at the amplitude dispersion of each pixel through the entire time-series. Only pixel with low amplitude dispersion can be PS. We therefore identified these potential PS for all three tracks (T9, T111, T147) between 2015 and 2024 for Krafla and Bjarnarflag and between 2017 and 2024 for Þeistareykir, when most pipelines were completed.

Results for Krafla, Bjarnarflag, and Þeistareykir are visible on Figures 19, 20, 21, respectively. They show that very few PS are identified in the geothermally altered areas. Some are found around well heads but almost none along the pipelines. Moreover, it is expected that some of these PS are actually not good PS. For example, at this stage of the processing some PS are also found over water bodies and they are definitely not actual PS. PS are usually dropped during a full PS-InSAR analysis after looking at the PS phase stability though time. Therefore, it is unlikely that doing a full PS-InSAR analysis of the Sentinel-1 data would significantly improve the retrieval of signal over the geothermally altered areas. Higher resolution data might be able to retrieve more signal, especially along the pipeline. But there are no guarantee of this and such high resolution data is provided by other satellite constellations which do not have an open data policy like Sentinel-1.

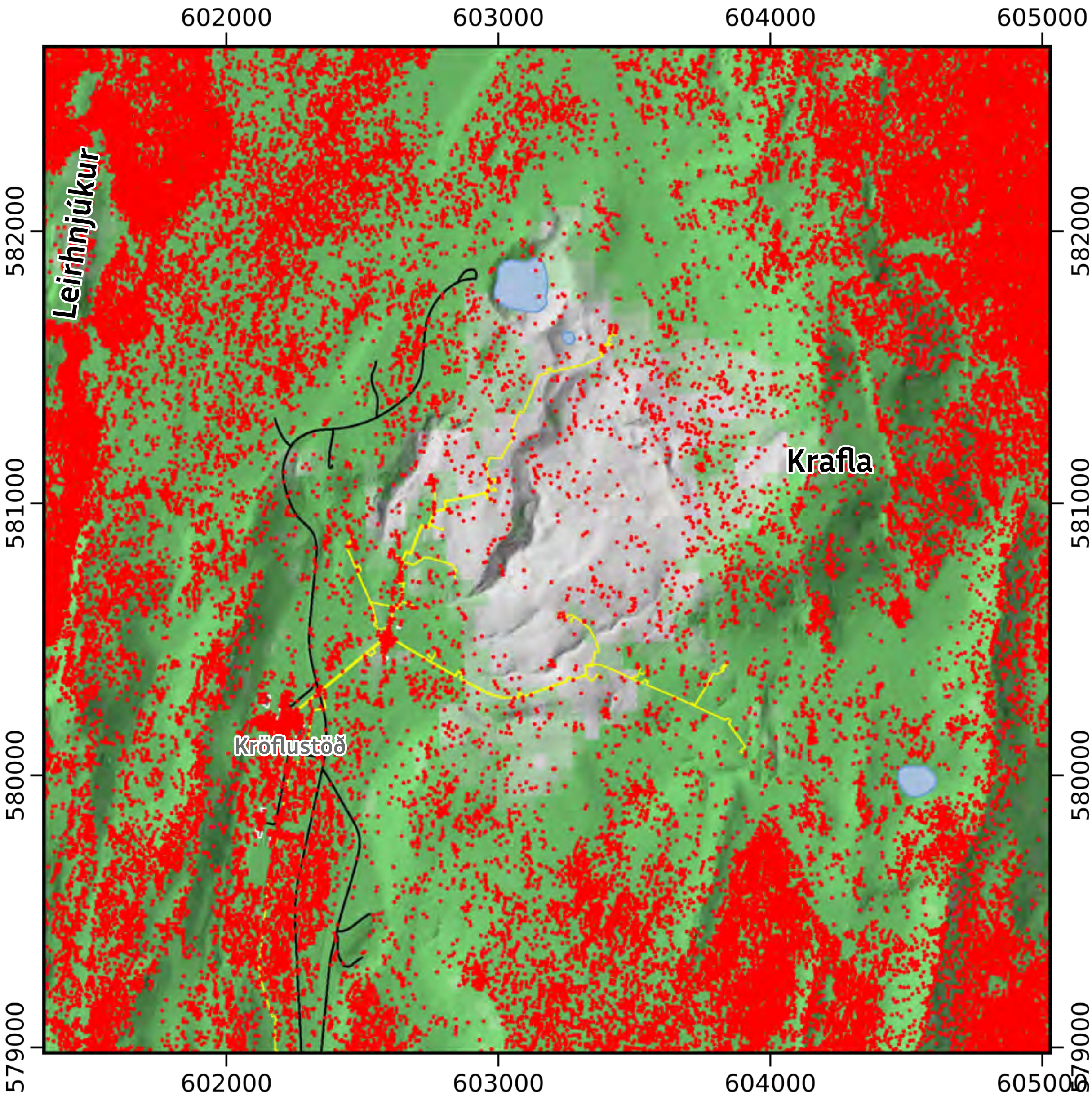

Figure 19: Map showing all the permanent scatterers (red points) found using amplitude dispersion analysis of all the three Sentinel-1 tracks (T9, T111, T147) over Krafla for 2015-2024. Green areas show where deformation signal is retrieved using the SBAS technique in this report, from one track (light green) to three tracks (dark green). Background shows shaded topography, roads (black lines), pipelines (yellow lines), buildings (dark grey areas), and water (blue areas). Background data partially from Landmælingar Íslands and OpenStreetMap contributors.

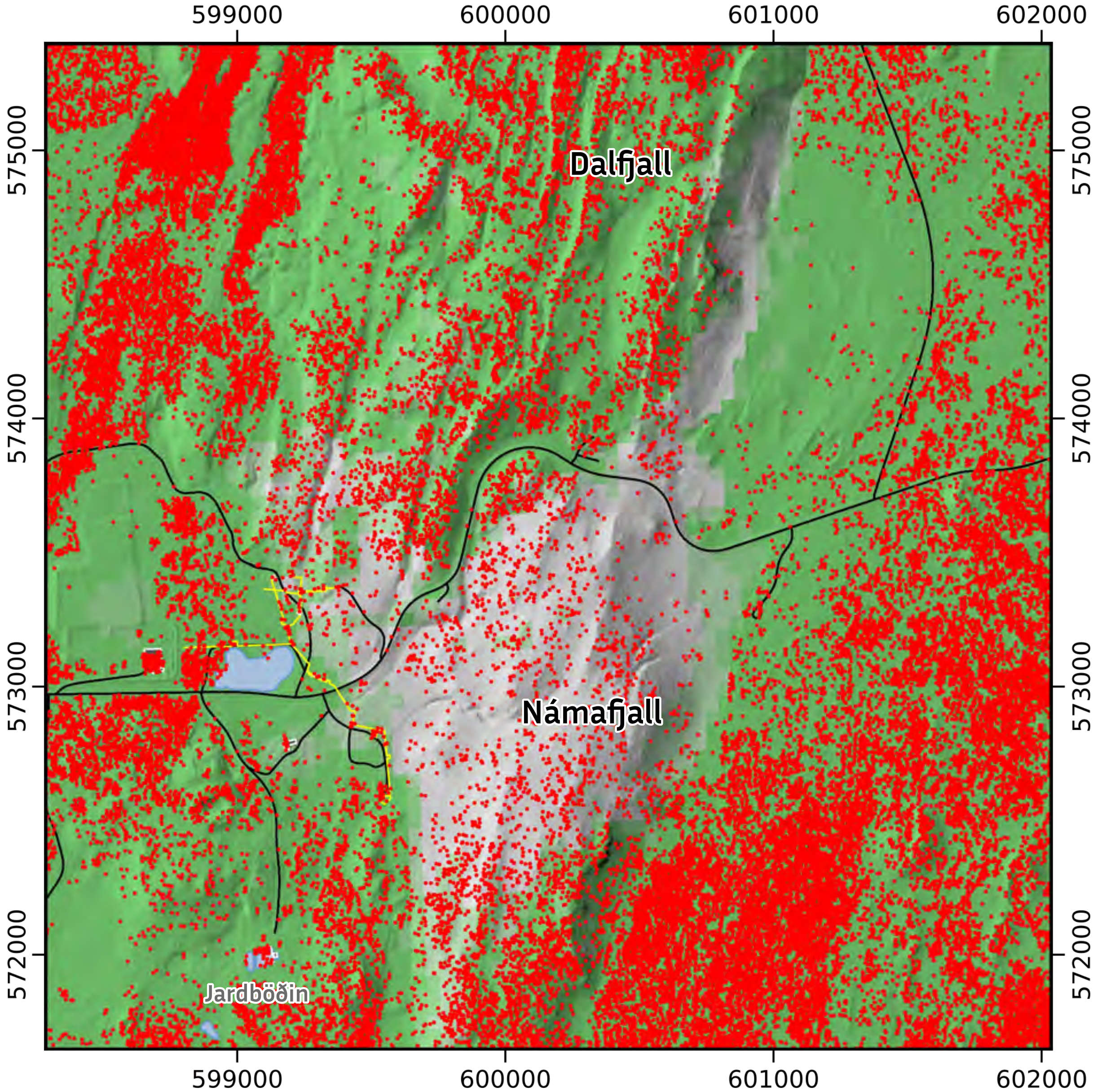

Figure 20: Map showing all the permanent scatterers (red points) found using amplitude dispersion analysis of all the three Sentinel-1 tracks (T9, T111, T147) over Bjarnarflag for 2017-2024. Green areas show where deformation signal is retrieved using the SBAS technique in this report, from one track (light green) to three tracks (dark green). Background shows shaded topography, roads (black lines), pipelines (yellow lines), buildings (dark grey areas), and water (blue areas). Background data partially from Landmælingar Íslands and OpenStreetMap contributors.

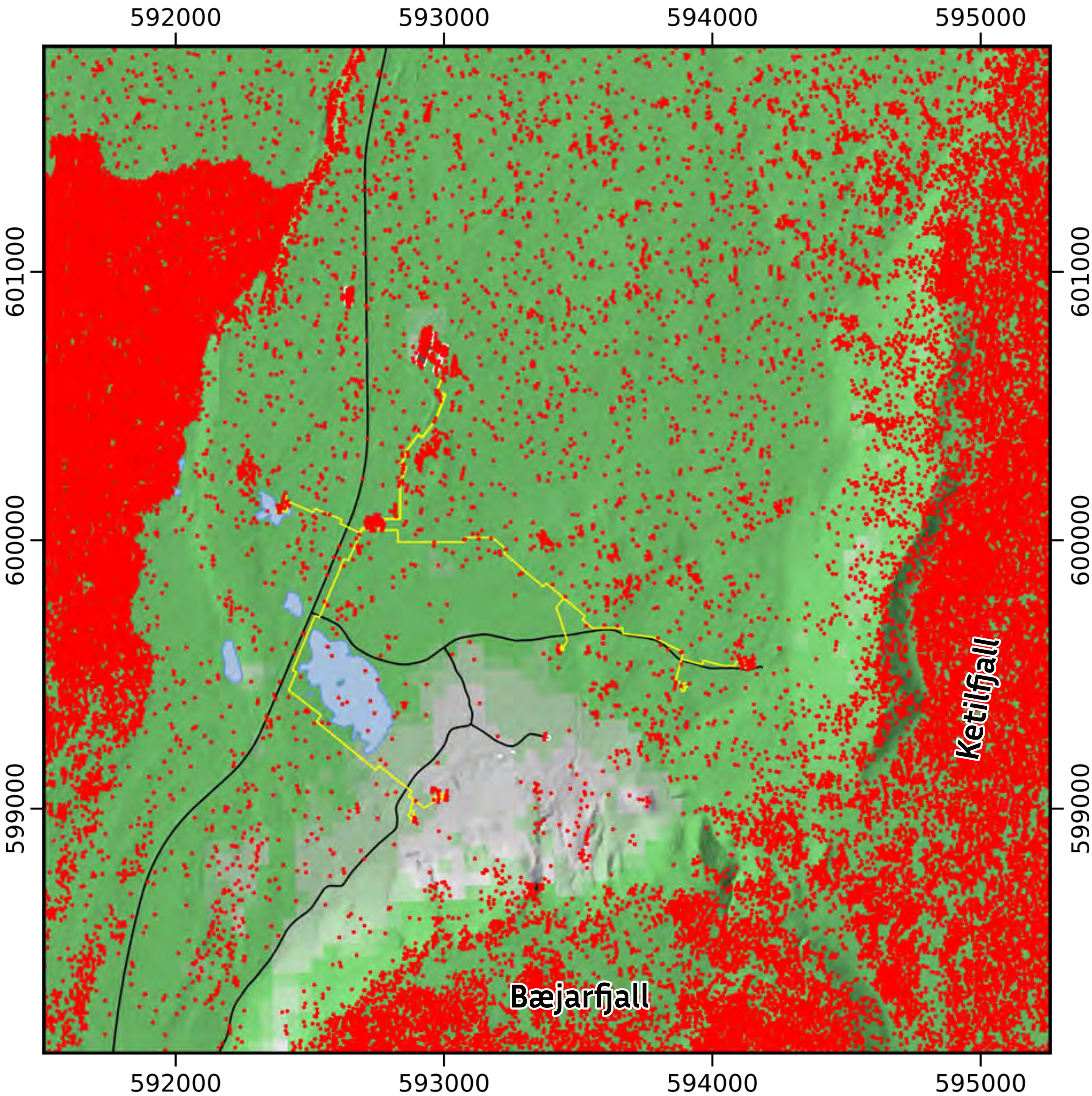

Figure 21: Map showing all the permanent scatterers (red points) found using amplitude dispersion analysis of all the three Sentinel-1 tracks (T9, T111, T147) over Þeistareykir for 2015-2024. Green areas show where deformation signal is retrieved using the SBAS technique in this report, from one track (light green) to three tracks (dark green). Background shows shaded topography, roads (black lines), pipelines (yellow lines), buildings (dark grey areas), and water (blue areas). Background data partially from Landmælingar Íslands and OpenStreetMap contributors.

4 Discussion

At Krafla, the deformation pattern shows a relatively fast subsidence (∼15 mm) in the center of the caldera between summer 2023 and summer 2024. This is a faster subsidence than the one observed during 2015-2018 deformation (Fig. 2). It appears to be located slightly to the south-east of the 2018-2019 main uplift. It is not possible to determine what source is behind this subsidence using deformation measurements alone. However, it would be good to check if this deformation signal is also visible on GNSS campaign measurements. Combining this deformation dataset with seismic measurements, gravimetry measurements, and extraction/injection data might help to narrow the list of potential explanations for these variations of the local deformation.

At Hvíthólar, subsidence is observed. In the previous years, subsidence appeared to correlate with geothermal fluid extraction at the local borehole KJ-21 (Drouin, 2022).

At Bjarnarflag, the deformation pattern is the same since at least 1993 (Drouin et al., 2017). There is a $\sim$6 mm/yr subsidence bowl centered a few hundred meters west of the power plant. Geothermal fluids extraction from local boreholes has been relatively stable since deformation measurements have been conducted in the area. Therefore, assuming the observed deformation is related to this extraction rate, this would explain why the deformation rate is stable through time.

At the Þeistareykir geothermal field and its vicinity, the main deformation pattern is the same since the start of production in 2017. There is a $<$5 mm/yr subsidence area between Bæjarfjall and the power plant. This deformation is likely related to the geothermal fluid extraction from all the boreholes. The subsidence on the top of Bæjarfjall as accelerated since 2022, from 2 mm/yr to 7-8 mm/yr. It would be interesting to check if this change correlates with changes in geothermal fluid extraction at the nearby boreholes. The subsidence is the fastest (10-15 mm/yr) near the injection boreholes. There, the accumulated subsidence is more than 80 mm since 2017. This subsiding area is about 1000 m long and 500 m wide, elongated along the fissure swarm direction. This suggest that the source of this deformation is shallow ($<$ 1 km deep). The injection boreholes are about 400 m deep. Therefore it is likely that this local subsidence is related to the re-injection of geothermal fluids. However, the mechanisms behind this process are unclear as uplift, not subsidence, is usually expected from re-injection (Juncu et al., 2020). Potential explanations include i) fast cooling and contraction of the host rock by the cold re-injected fluids ii) chemical dissolution of a geological layer sensitive to water.

At the Þeistareykir central volcano, a broad uplift is observed between summer 2022 and summer 2024. Two previous uplift episodes (1995-1996 and 2006-2009) have been observed since the beginning of geodetic measurement in the area (Metzger and Jónsson, 2014). The 1995–1996 deformation was 18 mm LOS and the 2006–2009 deformation was 78 mm LOS. For 2022-2024 the uplift is estimated to be $\sim$10-12 mm/yr using InSAR. Measurements from the continuous GNSS site THRC indicate that the uplift took place over one year and that it has stopped since the end of 2023. This means that the uplift rate from InSAR becomes $\sim$20-24 mm over one year. The uplift rate was therefore fairly similar for all three inflation events at $\sim$18-26 mm/yr.

References

Berardino, P., Fornaro, G., Lanari, R., & Sansosti, E. (2002). A new algorithm for surface deformation monitoring based on small baseline differential SAR interferograms. *IEEE Transactions on Geoscience and Remote Sensing*, *40*(11), 2375–2383. https://doi.org/10.1109/TGRS.2002.803792

Drouin, V. (2020). *InSAR Monitoring of Krafla, Bjarnarflag and Þeistareykir Geothermal Areas.* (tech. rep. No. ÍSOR-2020/43).

Drouin, V. (2022). *InSAR Monitoring of Krafla, Bjarnarflag and Þeistareykir Geothermal Areas, 2022 update.* (tech. rep. No. 22-001).

Drouin, V. (2023). *InSAR Monitoring of Krafla, Bjarnarflag and Þeistareykir Geothermal Areas, 2023 update.* (tech. rep. No. 23-001).

Drouin, V., & Sigmundsson, F. (2019). Countrywide Observations of Plate Spreading and Glacial Isostatic Adjustment in Iceland Inferred by Sentinel-1 Radar Interferometry, 2015–2018. *Geophysical Research Letters*, *46*(14), 8046–8055. https://doi.org/10.1029/2019GL082629

Drouin, V., Sigmundsson, b., Verhagen, S., Ófeigsson, B. G., Spaans, K., & Hreinsdóttir, S. (2017). Deformation at Krafla and Bjarnarflag geothermal areas, Northern Volcanic Zone of Iceland, 1993-2015 [Volcano Geodesy: Recent developments and future challenges]. *Journal of Volcanology and Geothermal Research*, *344*, 92–105. https://doi.org/10.1016/j.jvolgeores.2017.06.013

Einarsson, P. (1991). Umbrotin við Kröflu 1975-89. In A. Garðarsson & A. Einarsson (Eds.), *Náttúra Mývatns* (pp. 96–139). Hið íslenska náttúrufræðifélag.

Ferretti, A., Prati, C., & Rocca, F. (2000). Nonlinear subsidence rate estimation using permanent scatterers in differential sar interferometry. *IEEE Transactions on Geoscience and Remote Sensing*, *38*(5), 2202–2212. https://doi.org/10.1109/36.868878

Ferretti, A., Prati, C., & Rocca, F. (2001). Permanent scatterers in sar interferometry. *IEEE Transactions on Geoscience and Remote Sensing*, *39*(1), 8–20. https://doi.org/10.1109/36.898661

Juncu, D., Árnadóttir, T., Geirsson, H., Guðmundsson, G., Lund, B., Gunnarsson, G., Hooper, A., Hreinsdóttir, S., & Michalczewska, K. (2020). Injection-induced surface deformation and seismicity at the Hellisheidi geothermal field, Iceland. *Journal of Volcanology and Geothermal Research*, *391*, 106337. https://doi.org/10.1016/j.jvolgeores.2018.03.019

Metzger, S., & Jónsson, S. (2014). Plate boundary deformation in North Iceland during 1992–2009 revealed by InSAR time-series analysis and GPS. *Tectonophysics*, *634*, 127–138.

Rosen, P. A., Gurrola, E., Sacco, G. F., & Zebker, H. (2012). The InSAR scientific computing environment. *Synthetic Aperture Radar, 2012. EUSAR. 9th European Conference on*, 730–733.

Sturkell, E., Sigmundsson, F., Geirsson, H., Ólafsson, H., & Theodórsson, T. (2008). Multiple volcano deformation sources in a post-rifting period: 1989–2005 behaviour of Krafla, Iceland constrained by levelling, tilt and GPS observations. *Journal of Volcanology and Geothermal Research*, *177*(2), 405–417. https://doi.org/10.1016/j.jvolgeores.2008.06.013

A Appendix

A.1 Krafla & Bjarnarflag

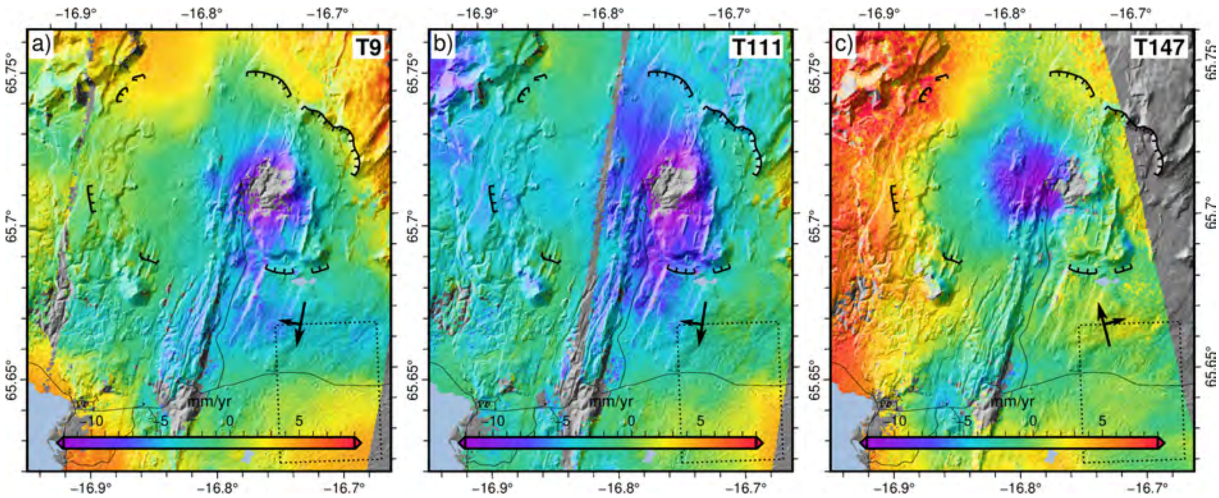

Figure 22: Average LOS velocities between summer 2023 and summer 2024 for all three Sentinel-1 track covering the area. Satellite heading and look direction is indicated by the large arrow and the small arrow, respectively. Background show shaded topography, the Krafla caldera boundary (comb line), roads (thin lines), and lakes (blue areas).

A.2 Þeistareykir

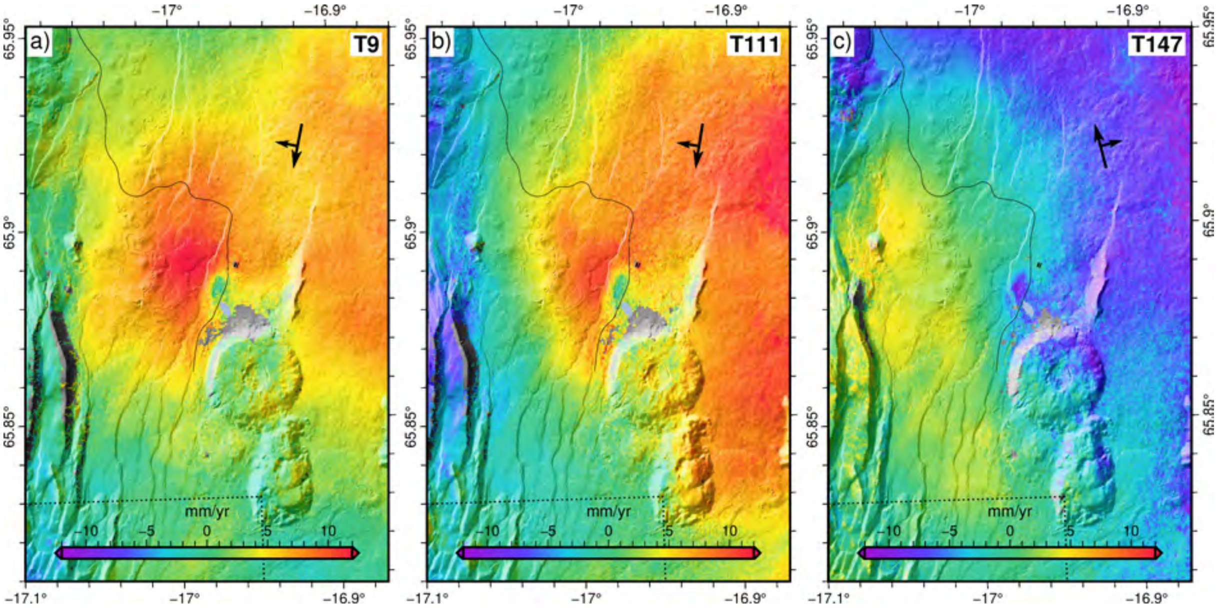

Figure 23: Average LOS velocities between summer 2023 and summer 2024 for all three Sentinel-1 track covering the area. Satellite heading and look direction is indicated by the large arrow and the small arrow, respectively. Background show shaded topography and roads (thin lines).

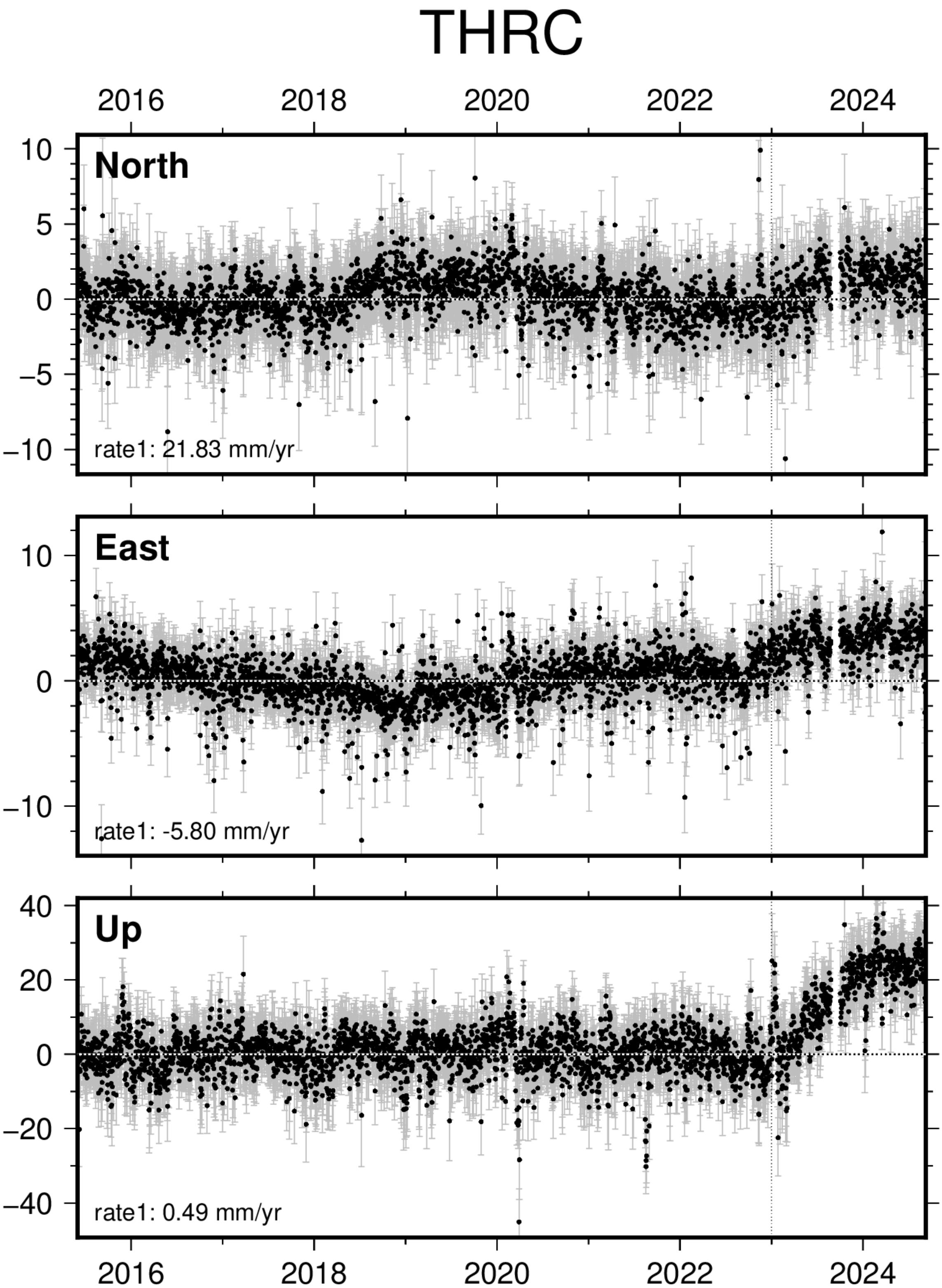

Figure 24: Time-series of the THRC continuous GNSS station. The time-series are detrended from the base rate until the end of 2022 (vertical dotted line) and the annual cycle to emphasize the uplift happening in 2023.